A Novel Hybrid Modeling Method for Predicting Energy Use of Hydronic Radiant Slab Systems

Lichen Wu[1], Liping Wang[1]*, James Braun[2]

[1]Department of Civil and Architectural Engineering, University of Wyoming,
Laramie, WY, 82071, United States
lwang12@uwyo.edu

[2]School of Mechanical Engineering, Purdue University,
West Lafayette, IN 47907-2088, United States

* Corresponding Author

ABSTRACT

Accurately predicting the performance of radiant slab systems can be challenging due to the large thermal capacitance of the radiant slab and room temperature stratification. Current methods for predicting heating and cooling energy consumption of hydronic radiant slabs include detailed first-principles (e.g., finite difference) and reduced-order (e.g., thermal Resistor-Capacitor (RC) network) models. Creating and calibrating detailed first-principles models, as well as detailed RC network models for predicting the performance of radiant slabs require substantial effort. To develop improved control, monitoring, and diagnostic methods, there is a need for simpler models that can be readily trained using in-situ measurements.

In this study, we explored a novel hybrid modeling method that integrates a simple RC network model with an evolving learning-based algorithm termed the Growing Gaussian Mixture Regression (GGMR) modeling approach to predict the heating and cooling rates of a radiant slab system for a Living Laboratory office space. The RC network model predicts heating or cooling load of the radiant slab system that is provided as an input to the GGMR model. Three modeling approaches were considered in this study: 1) an RC network model; 2) a GGMR model, and 3) the proposed hybrid modeling between RC and GGMR. The three modeling methods have been compared for predicting the energy use of a radiant slab system of a Living Laboratory office space using measurement data from January 15th to March 7th, 2022. The first two weeks of data were used for training, while the remaining data was used for testing of all three modeling methods. The hybrid approach had a Normalized Root Mean Square Error (NRMSE) of 8.77 percent (4.79 percent less than the RC and 11.98 percent less than GGMR models), a Coefficient of Variation of RMSE (CVRMSE) of 9.95 percent (5.64 percent less than the RC and 12.6 percent less than the GGMR), a Mean Absolute Error (MAE) of 3.62 kW (2.14 kW less than the RC and 3.99 kW less than the GGMR), and a Mean Absolute Percentage Error (MAPE) of 19.31 percent (89.22 percent lower than the RC, 8.43 percent lower than the GGMR). The hybrid modeling approach significantly outperformed both the RC and GGMR models.

1. INTRODUCTION

Hydronic radiant slab systems (HRSS) have significant benefits for thermal management of conditioned spaces, including increased thermal comfort and energy savings (Joe and Karava 2019; Rhee and Kim 2015). Apart from these benefits, the large thermal storage capacity of an HRSS has a few disadvantages. One disadvantage of the large thermal time constant is that it causes cooling output to be delayed when supply water flow rates and temperature are adjusted (Liu et al. 2011). Additionally, conventional control based on room temperature feedback may consume more primary energy than a conventional air system (Sourbron et al. 2009). Moreover, an HRSS frequently experiences concurrent thermal disturbances caused by solar radiation, internal heat, and air systems (Koschenz and Dorer 1999) that when combined with conventional control approaches can lead to overcooling or overheating issues. To address these issues, an HRSS should incorporate Model Predictive Control (MPC) with accurate load prediction (Joe and Karava 2019). In general, load prediction methods for buildings fall into three categories: first-principles models, reduced-order thermal Resistor-Capacitor (RC) network models, and data-driven

models, as summarized in ASHRAE (Handbook 2001) and (Dong et al. 2016). The following subsections will review those models followed by a brief statement of research objectives.

1.1 First-Principles Models

In this application, first-principles models refer to models that use Computational Fluid Dynamics (CFD) (Zhang et al. 2013) or building energy simulation software such as EnergyPlus (Crawley et al. 2001), and ESP-r (Clarke 2001). The computational cost of CFD makes them incompatible with large-scale simulation programs (Neumann, Gamisch, and Gschwander 2021; Rodríguez Jara et al. 2016). Most current building energy software requires a detailed physical and operational description of the building, as well as a well-mixed zone air assumption, to predict the performance of a building and its heating, ventilation, and air conditioning (HVAC) system.

1.2 Thermal RC Network Models

An inverse grey-box RC model strikes a balance between a physically-based model and a data-driven model (Braun and Chaturvedi 2002). An RC network model is considered as a collection of linear ordinary differential equations (ODEs). RC models are typically in the form of 2R1C, 3R2C, or lumped RC parameter models with associated self-adjusting methods (Rodríguez Jara et al. 2016). According to (O'Dwyer et al. 2016), when the resistance and capacitance values are positive, there is theoretically a guaranteed thermal passivity solution for RC models. As for the training of RC models, there is considerable research devoted to optimizing the trade-off between model accuracy and complexity (Ahn and Song 2010; Goyal, Liao, and Barooah 2011; Koschenz and Dorer 1999; Liu et al. 2011).

Nevertheless, there are some limitations in terms of the application of the RC model. The accuracy of lumped parameter methods is highly dependent on the estimation and calibration of their characteristic parameters (Rodríguez Jara et al. 2016), which requires substantial effort. Moreover, the accuracy of the RC model applied to a radiant slab degrades when the slab is subjected to rapid thermal disturbances (Neumann, Gamisch, and Gschwander 2021; Rhee and Kim 2015).

1.3 Data-driven Models

Many data-driven/machine learning algorithms have been evaluated for building energy models such as Partial Least Squares (PLS), Principal Component Analysis (PCA), Gaussian Process Regression (GPR) and Gaussian Mixture Model (GMM). For example, GPR has been used to capture the complex and highly subjective relationships between room temperature and subjective thermal perception (Guenther and Sawodny 2019). Also, GMM is widely recognized for its ability to model multimode characteristics and deal with process uncertainty (Billard et al. 2008; Li and Song 2020).

Considerable efforts have been made in the field of incremental learning Gaussian Mixture Regression (GMR), or Growing GMR (GGMR), to develop a mechanism for GMR adaptation (Bouchachia and Vanaret 2011; Cederborg et al. 2010; Karami and Wang 2018; Li and Song 2020; Wang, Kubichek, and Zhou 2018).

In this study, we propose a hybrid approach, in which the output from a simpler RC model is used as one of the inputs to a GGMR model. The proposed hybrid model combines the benefits of both the GGMR and RC models. The methodology and performance metrics for model evaluation are detailed in Section 2. Section 3 presents model development and a case study for an existing office at Purdue University followed by conclusions in Section 4.

2. METHODOLOGY

This section discusses the development of RC network models, the GGMR approach, and the hybrid modeling approach along with describing the model prediction performance criteria metrics.

2.1 RC Network Model

An RC network model is based on heat balance equations applied to temperature state variables (Braun and Chaturvedi 2002; Joe and Karava 2017). A general state-space model for estimating a radiant slab systems load is of the form

$$\frac{x}{dt} = A\mathrm{x} + \mathrm{Bu} \tag{1}$$

$$y = c^T x + d^T u$$

where estimated resistances, capacitances and heat flux coefficients (such as the ratio of solar radiation to the envelope state) form matrices *A, B* and vectors *c*, *d*. The variables *x, u, y, t* represent vectors of state, input, output variable and sampling time, respectively. For an HRSS, a single output variable is the cooling and heating load. The state vector contains all the temperature nodes. The input vector contains all the driving conditions, such as the heating or chilled water temperature, exterior air temperature, solar radiation, lighting, and occupancy schedule. The discrete version of the above state-space model can be written in terms of a recursive formula as

$$x_{(k+1)T} = A_d x_{kT} + B_d u_{kT} \quad (2)$$

$$y_{kT} = {c_d}^T x_{kT} + {d_d}^T u_{kT} \quad (3)$$

where the subscript *d* indicates these variables are the discretized forms of *A, B, c, d* in equation (1). A typical objective function for training an RC network model is to minimize the Root-Mean-Square Error (RMSE) for the training duration, denoted as the following, where *N* stands for the number of samples.

$$minimize \sqrt{\frac{\sum_{k=1}^{N_{train}} \left(y_{measured,k} - y_{predicted,k}\right)^2}{N_{train} - 1}} \quad (4)$$

2.2 GGMR Method

GMR(Sung 2004) is a regression approach that models probability distributions rather than functions. Assume the data follow the joint density

$$f_{X,Y}(x,y) = \sum_{j=1}^{K} \pi_j \, \phi\left(x, y; \mu_j, \Sigma_j\right) \quad (5)$$

where K is the number of Gaussian mixtures, π_j is the weight coefficient mean $\mu_j = \begin{bmatrix} \mu_{jX} \\ \mu_{jY} \end{bmatrix}$, covariance $\Sigma_j = \begin{bmatrix} \Sigma_{jX} & \Sigma_{jY} \\ \Sigma_{YX} & \Sigma_{YY} \end{bmatrix}$. The Gaussian mixture probability function shown in equation (5) can be presented as

$$f_{X,Y}(x,y) = \sum_{j=1}^{K} \pi_j \, \phi\left(y|x; m_j(x), \sigma_j^2\right) \phi\left(x; \mu_{jX}, \Sigma_{jX}\right) \quad (6)$$

where

$$m_j(x) = \mu_{jX} + \Sigma_{jYX} \Sigma_{jX}^{-1} \left(x - \mu_{jX}\right) \quad (\textbf{Error! Bookmark not defined.}7)$$

$$\sigma_j^2 = \Sigma_{jYY} - \Sigma_{jYX} \Sigma_{jx}^{-1} \Sigma_{jXY} \quad (\textbf{Error! Bookmark not defined.}8)$$

From equation (6), the marginal density of X is

$$f_X(x) = \sum_{j=1}^{K} \pi_j \, \phi\left(x; \mu_{jX}, \Sigma_{jX}\right) \quad (\textbf{Error! Bookmark not defined.}9)$$

The conditional probability density function of $Y|X$ is

$$f_{Y|X}(y|x) = \sum_{j=1}^{K} w_j(x) \, \phi\left(y; m_j(x), \sigma_j^2\right) \quad (10)$$

with the mixing weight

$$w_j(x) = \frac{\pi_j \phi\left(x; \mu_{jx,\Sigma_{jX}}\right)}{\sum_{j=1}^{K} \pi_j \, \phi\left(x; \mu_{jX}, \Sigma_{jX}\right)} \tag{11}$$

In the current study, we are interested in the expectation of y among all gaussian components:

$$y_{predicted|x} = m(x) = E[Y|X = x] = \sum_{k=1}^{K} w_j(x) m_j(x) \tag{12}$$

To accommodate new data in an online setting, control model complexity and allow modeling of time-varying processes, GGMR has been proposed by (Bouchachia and Vanaret 2011) with growing and shrinking mechanisms. We utilized its updating Gaussians algorithm in the present paper. More details can be seen in (Bouchachia and Vanaret 2011). The best match Gaussian is updated using the following formulas:

$$q_j = \frac{p_j}{\sum_{k=1\ldots K} p_k} \tag{13}$$

$$c_j(t) = c_j(t-1) + q_j \tag{14}$$

$$\tau_j(t) = (1-\alpha)\tau_j(t-1) + \alpha q_j \tag{15}$$

$$\eta_j = q_j\left(\frac{1-\alpha}{c_j} + \alpha\right) \tag{16}$$

$$\mu_j(t) = \left(1-\eta_j\right)\mu_j(t-1) + \eta_j x_i \tag{17}$$

$$\Sigma_j(t) = \left(1-\eta_j\right)\Sigma_j(t-1) + \eta_j\left(x_i - \mu_j(t-1)\right)^2 \tag{18}$$

in which p_j is the match probability calculated with new input x_i and best match Gaussian $\phi_j\left(\mu_j, \Sigma_j\right)$, q_j is the expected posterior, c_j is the sum of the expected posterior for the best match Gaussian, τ_j are the weights of the best match Gaussian, η_j is the on-going learning rate for the j-th Gaussian, α is the converging learning rate.

2.3 Hybrid Approach

In the present study, we have designed the hybrid modeling approach schema as shown in Figure **1**, which illustrates the underlying structure of the hybrid approach. For each timestamp, the real-time predicted load from the RC model is used as one of inputs for the GGMR model (equations (13) – (18)). GGMR predicts system performance by updating key GMM parameters such as weighting factors, mean vectors, and covariance matrices. Sec. 3 described the detailed hybrid model inputs. In practice, the trained RC model should be started with a reasonable estimate of the initial states. As a result of non-optimal state initialization, it is expected that the first few predictions from the RC model will be chaotic. The current study proposed a warming-up period to minimize the errors caused by imperfect states initialization, and subsection 3.3 detailed how the warming-up steps were determined.

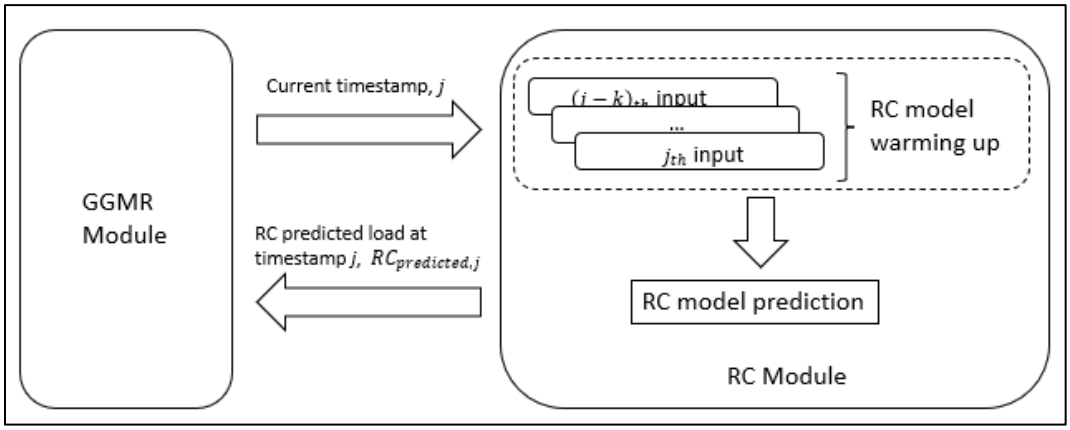

Figure 1 Underlying communication for hybrid approach.

2.4 Model Performance Evaluation Criteria

Four indices, Normalized Root Mean Square Error (NRMSE), Coefficient of Variation of RMSE (CVRMSE), and Mean Absolute Error (MAE), and Mean Absolute Percentage Error (MAPE), are used for model performance evaluation.

$$RMSE = \sqrt{\frac{\sum_{k=1}^{n}\left(y_{measured,k} - y_{predicted,k}\right)^2}{n-1}} \tag{19}$$

$$\text{NRMSE} = \frac{RMSE}{s\left(y_{predicted}\right)} \tag{20}$$

$$\text{CVRMSE} = \frac{RMSE}{\bar{y}_{measured}} \tag{21}$$

$$MAE = \frac{\sum abs\left(y_{measured,k} - y_{predicted,k}\right)}{n} \tag{22}$$

$$MAPE = \frac{1}{n}\sum abs\left(\frac{y_{measured,k} - y_{predicted,k}}{y_{measured,k}}\right) \tag{23}$$

where n is the number of observations, $s\left(y_{predicted}\right)$ is the standard deviation of predictions, and $\bar{y}_{measured}$ is the average of measured values.

3. CASE STUDY

This section presents a case study that investigates the performance of the RC, GGMR and hybrid modeling approaches.

3.1 Testbed

The dataset included in-situ measurements for a living laboratory office space from January 15th to March 7th, 2022, with a 5-minute sampling rate. The first two weeks of data were used for training and the rest of the data was used for testing. The dataset was divided into two categories, onsite sensor data and estimated data. Onsite sensor data includes the following: outdoor air temperature denoted by T_{out}, façade cavity space temperature denoted by T_{cav}, slab concrete temperature denoted by T_{slab}, flowing water temperature within slab pipe denoted by T_{source}, solar radiation retrieved from a weather station denoted by $\dot{Q}_{solar}$(Ambient Weather Network 2022), and Air Handling Unit (AHU) consumed heating power $\dot{Q}_{AHU}$. The estimated input values were determined using hourly schedules in accordance with (ANSI/ASHRAE/IES 90.1-2010 2010, 1), such as internal heating radiation denoted by $\dot{Q}_{int}$ based on occupancy schedule, and lighting radiation $\dot{Q}_{light}$ based on lighting schedule.

3.2 RC Network Model Development

This subsection describes the design logic for the RC model, followed by a description of the target room's physical structures and, finally, our consideration of various RC model designs and their associated performance. Ultimately, the chosen design will be detailed.

The major thermal components of the living laboratory office space include external walls, roof/ceiling, internal wall, south-facing double façade system, conditioned air from AHU system, and hydronic radiant floor system. Generally, adding complexity to an RC model can improve accuracy over a wide range of operating conditions, but at the expense of requiring additional input variables and more training data. In the present study, we considered three RC network designs by considering model robustness and various levels of complexity or model orders. As illustrated in Figure **2**, the three RC network models considered are a four-state Model 1, a five-state Model 2 and a six-state Model 3. In these network diagrams, T, C, Q, α represent temperatures, capacitances, resistances, heat fluxes and corresponding coefficients, whereas the subscripts, $out, cav, slab, source, sink, env, room, intwall, sol, int, light, AHU, rad$, represent outdoor air, façade cavity, slab concrete, hot water or chilled water within tubes, insulation below tubes, envelope, room air, internal wall, solar radiation, internal heat, lighting, air handling unit, and thermal heat flux load requirements, respectively.

Each of the three models is composed of two components: room and concrete slab. We chose the same RC network model for the room portion of the model to effectively capture its thermal properties: a two-node envelope, one-node internal wall, one node cavity for the double façade system, and a room air node to capture disturbances due to heating or cooling from the AHU system. It is worth noting that we used the envelope node to represent the external wall and roof/ceiling to keep the model simple. For the concrete slab portion of the model, we experimented with various model orders. The detailed thermal structure of the radiant floor was omitted from Model 1 and we considered the entire slab to be a single node. In comparison to Model 1, Model 2 included an additional source node to represent the flow of water through slab pipes. Furthermore, Model 3 had one additional sink node compared to Model 2 to represent heat transfer between the source node and another space.

Figure **3** depicts predicted and actual results obtained for the testing period (10656 sampling points for 37 days). Model 1 has significantly higher errors than Models 2 and 3, which can be attributed to the oversimplified concrete slab representation. Model 3 has a lower CVRMSE than Model 2, which is consistent with the addition of a sink node. Table **2** contains a more detailed comparison of performance.

The Model 2 can be represented by a state-space model with the following state, input, and output variable definitions:

$$\boldsymbol{x}^T = [T_{env1}, T_{env2}, T_{room}, T_{intwall}, T_{slab2}, T_{sink}] \tag{24}$$

$$\boldsymbol{u}^T = \left[T_{out}, T_{slab1}, T_{cav}, T_{source}, \dot{Q}_{sol}, \dot{Q}_{int}, \dot{Q}_{light}, \dot{Q}_{AHU}, \frac{dT_{source}}{dt}\right] \tag{25}$$

$$\mathrm{y} = \dot{Q}_{rad} \tag{26}$$

As stated in equation (4), the RC network model training is essentially an optimization problem to determine those unknown resistances, capacitances, and heat flux coefficients. The final converged values for those learning parameters have been listed in Table **1**. In the present paper, Particle Swarm Optimization (PSO) from python package (James V. Miranda 2018) was used to solve the above optimization problem.

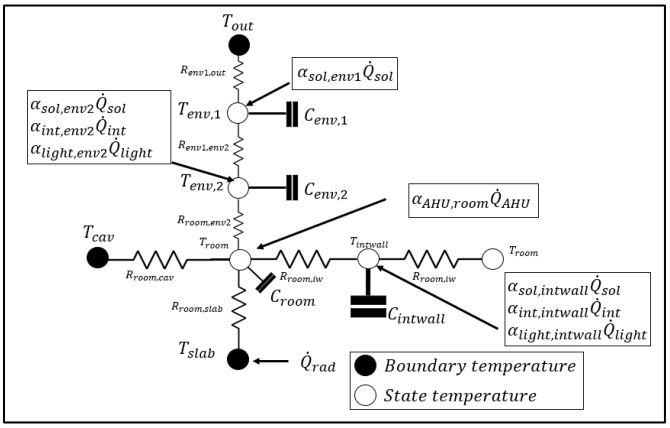

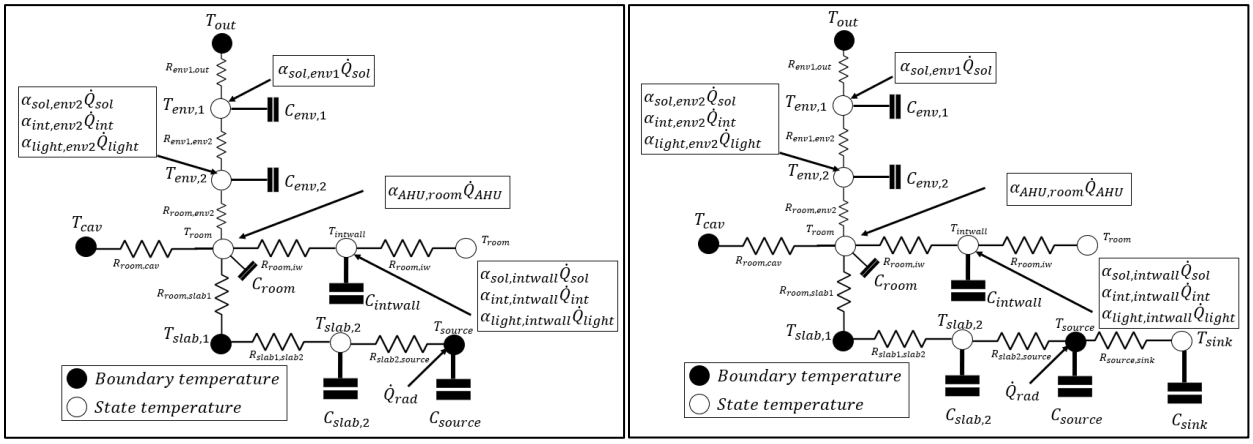

Figure 2 Structure of RC network. Top: four states Model 1; Left: five states Model 2; Right: six states Model 3.

Table 1 Final converged values of resistances (K/W), capacitances (J/K) and heat flux coefficients for Model 3.

$R_{out,env1} = 3.11E\text{-}1$	$R_{env2,env1} = 5.45E\text{-}1$	$R_{env2,room} = 9.94E\text{-}1$	$R_{intwall,room} = -1.46E\text{-}2$
$R_{slab1,room} = 7.21E\text{-}1$	$R_{cav,room} = 4.69E\text{-}1$	$R_{slab1,slab2} = 5.64E\text{-}4$	$R_{source,slab2} = 6.44E\text{-}4$
$R_{source,sink} = 9.07E\text{-}4$	$C_{env1} = 2.6E6$	$C_{env2} = 1.3E6$	$C_{room} = 1E8$
$C_{iw} = 1.2E6$	$C_{slab2} = 6E6$	$C_{sink} = 2E4$	$C_{source} = 2.75E5$
$\alpha_{sol,env1} = 1E2$	$\alpha_{sol,env2} = 1.87E\text{-}1$	$\alpha_{int,env2} = 1.52$	$\alpha_{light,env2} = 2.46$
$\alpha_{AHU,room} = 1.41$	$\alpha_{sol,intwall} = 4.66E\text{-}1$	$\alpha_{int,intwall} = 1.01$	$\alpha_{light,intwall} = 1.78$

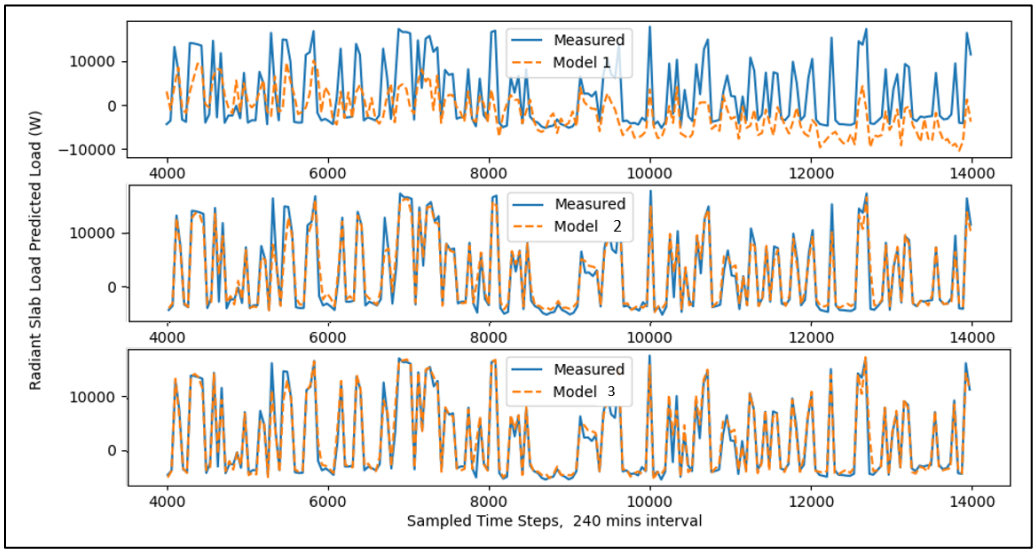

Figure 3 Testing results for Model 1, Model 2 and Model 3.

Table 2 Hourly prediction performance statistical comparison for proposed RC models.

Models	**NRMSE (%)**	**CVRMSE (%)**	**MAE (kW)**	**MAPE (%)**
Model 1	134.51	110.95	42.41	429.55
Model 2	16.89	17.80	6.89	**66.28**
Model 3	**13.56**	**15.59**	**5.76**	108.53

3.2 GGMR Model Development

This subsection primarily discusses the determination of the input variables for the GGMR model. Correlation coefficients R were used as an initial guess input variables. We experimented with various input combinations for the GGMR model. Table **3** shows example correlation coefficients for one of the cases considered, whereas the performance of the GGMR models with 3 different sets of inputs is shown in Table **4**. It is worth noting that larger correlation coefficients do not necessarily mean better prediction. For instance, the correlation coefficient of Q_{solar} is more significant than T_{out}, while the inputs including Q_{solar} did not provide additional prediction performance as shown in cases 1 and 2 of Table **4**. Moreover, it was found that better prediction performance is achieved if we provide flow rate information as an additional input. In comparison to case 1, case 3 had a 3.26% lower CVRMSE after adding $Flow_{Predicted,GGMR}$ from another GGMR prediction. In the end, the case 3 inputs were selected for the GGMR model.

Table 3 Correlation coefficients between radiant slab system load and input variables.

T_{out}	T_{slabs}	T_{cav}	$Valve_{cl}$	$Valve_{ht}$	Q_{solar}	$RadiantSlab_{load}$
-0.06	-0.08	-0.16	-0.89	0.35	-0.16	1

Table 4 Hourly prediction performance comparison for different GGMR inputs.

Case #	Inputs	CVRMSE (%)
1	$T_{out}, T_{slabs}, T_{cav}, Valve_{cl}, Valve_{ht}$	25.81
2	$\mathrm{T_{out}}, \mathrm{T_{slabs}}, \mathrm{T_{cav}}, \mathrm{Valve_{cl}}, \mathrm{Valve_{ht}}, Q_{solar}$	26.93
3	$T_{out}, T_{slabs}, T_{cav}, Valve_{cl}, Valve_{ht}, Flow_{Predicted,GGMR}$	**22.55**

3.3 Hybrid Model Development

As mentioned in Sec. 2.3, the development of the hybrid approach is primarily concerned with the determination of warming-up step for the RC model. As illustrated in Figure **4**, the warming up step was statistically chosen as 15 to minimize the prediction error. Consistent with GGMR model, different input combinations for the hybrid model were also investigated as presented in Table **5** where $RC_{predicted,RealTime}$ represents the predicted load from RC model. Compared with case 1, case 2 had 1.27% lower CVRMSE, which was consistent with the results shown in Table **4**. In the end, the case 2 inputs were selected for the hybrid model.

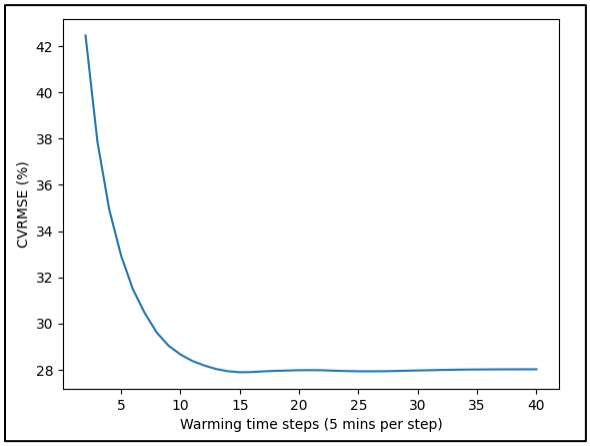

Figure 4 Determination of warming up step for RC model based on stepwise (5 minutes) prediction performance.

Table 5 Hourly prediction performance comparison for different hybrid model inputs.

Case #	Inputs	CVRMSE (%)

1	$T_{out}, T_{slabs}, T_{cav}, Valve_{cl}, Valve_{ht}, RC_{predicted,RealTime}$	11.22
2	$T_{out}, T_{slabs}, T_{cav}, Valve_{cl}, Valve_{ht}, Flow_{Predicted,GGMR}, RC_{predicted,RealTime}$	**9.95**

3.3 Performance Comparison for Proposed Models

Based on the statistical results presented in Table **5**, all three proposed models comply with ASHRAE Guideline 14 (ASHRAE 2014). Moreover, this table demonstrates that the hybrid model is the most accurate model for predicting the energy consumption of radiant slab systems, as it incorporates information from both the RC and GGMR models. Specifically, the hybrid approach has an NRMSE of 8.77 percent (4.79 percent less than the RC alone and 11.98 percent less than the GGMR alone), a CVRMSE of 9.95 percent (5.64 percent less than the RC and 12.6 percent less than the GGMR), an MAE of 3.62 kW (2.14 kW and 3.99 kW less than the RC and GGMR, respectively), and a MAPE of 19.31 percent (89.22 percent lower than the RC, and 8.43 percent lower than the RC and GGMR, respectively).

Table 5 Hourly prediction performance comparison of proposed models.

Models	NRMSE (%)	CVRMSE (%)	MAE (kW)	MAPE (%)
RC-Model 3	13.56	15.59	5.76	108.53
GGMR	20.75	22.55	7.61	27.74
Hybrid	**8.77**	**9.95**	**3.62**	**19.31**

4. CONCLUSIONS

In this paper, a novel hybrid modeling approach has been proposed to predict the energy consumption of a hydronic radiant slab system that incorporates the advantages of both RC and GGMR models. The hybrid approach involves using an output from one simplified RC model as an input to the GGMR. The proposed method was validated using measurements from a radiant slab system operating at Purdue University. According to the case study, the hybrid model significantly outperformed the RC and GGMR models in terms of prediction performance. The proposed hybrid model had a CVRMSE of 9.95 percent for hourly prediction (5.64 percent less than the RC alone and 12.6 percent less than GGMR alone), which clearly meets the criteria for ASHRAE Guideline 14.
In addition, it's worth noting that the case study makes use of a single onsite dataset source. In the future, we need to conduct additional case studies using a variety of data sources.

ACKNOWLEDGEMENT

This study was supported by the National Science Foundation Environmental Sustainability program under Grant No. 1929209. Any opinions, findings, and conclusions, or recommendations expressed in this material are those of the authors and do not necessarily reflect the views of the National Science Foundation.

REFERENCES

Ahn, Byung-Cheon, and Jae-Yeob Song. 2010. “Control Characteristics and Heating Performance Analysis of Automatic Thermostatic Valves for Radiant Slab Heating System in Residential Apartments.” *Energy* 35(4): 1615–24.

Ambient Weather Network. 2022. *Ambient Weather Network*. https://ambientweather.net/ (April 11, 2022).

ANSI/ASHRAE/IES 90.1-2010. 2010. *Energy Standard for Buildings Except Low-Rise Residential Buildings*. American Society of Heating, Refrigerating and Air-Conditioning Engineers.

ASHRAE. 2014. “ASHRAE Guideline 14: Measurement of Energy, Demand and Water Savings.” : 150.

Billard, Aude, Sylvain Calinon, Rüdiger Dillmann, and Stefan Schaal. 2008. "Robot Programming by Demonstration." In *Springer Handbook of Robotics*, eds. Bruno Siciliano and Oussama Khatib. Berlin, Heidelberg: Springer, 1371–94. https://doi.org/10.1007/978-3-540-30301-5_60 (April 12, 2022).

Bouchachia, Hamid, and Charlie Vanaret. 2011. "Incremental Learning Based on Growing Gaussian Mixture Models."

Braun, James E., and Nitin Chaturvedi. 2002. "An Inverse Gray-Box Model for Transient Building Load Prediction." *HVAC&R Research* 8(1): 73–99.

Cederborg, Thomas, Ming Li, Adrien Baranes, and Pierre-Yves Oudeyer. 2010. "Incremental Local Online Gaussian Mixture Regression for Imitation Learning of Multiple Tasks." In *2010 IEEE/RSJ International Conference on Intelligent Robots and Systems*, , 267–74.

Clarke, Joseph. 2001. *Energy Simulation in Building Design*. 2nd ed. London: Routledge.

Crawley, Drury B. et al. 2001. "EnergyPlus: Creating a New-Generation Building Energy Simulation Program." *Energy and Buildings* 33(4): 319–31.

Dong, Bing, Zhaoxuan Li, S. M. Mahbobur Rahman, and Rolando Vega. 2016. "A Hybrid Model Approach for Forecasting Future Residential Electricity Consumption." *Energy and Buildings* 117: 341–51.

Goyal, Siddharth, Chenda Liao, and Prabir Barooah. 2011. "Identification of Multi-Zone Building Thermal Interaction Model from Data." In *2011 50th IEEE Conference on Decision and Control and European Control Conference*, , 181–86.

Guenther, Janine, and Oliver Sawodny. 2019. "Feature Selection and Gaussian Process Regression for Personalized Thermal Comfort Prediction." *Building and Environment* 148: 448–58.

Handbook, ASHRAE. 2001. "Fundamentals SI Edition." *American Society of Heating, Refrigerating and Air-Conditioning Engineers, Inc., Atlanta, GA*.

James V. Miranda, Lester. 2018. "PySwarms: A Research Toolkit for Particle Swarm Optimization in Python." *The Journal of Open Source Software* 3(21): 433.

Joe, Jaewan, and Panagiota Karava. 2017. "Agent-Based System Identification for Control-Oriented Building Models." *Journal of Building Performance Simulation* 10(2): 183–204.

Karami, Majid, and Liping Wang. 2018. "Fault Detection and Diagnosis for Nonlinear Systems: A New Adaptive Gaussian Mixture Modeling Approach." *Energy and Buildings* 166: 477–88.

Koschenz, Markus, and Viktor Dorer. 1999. "Interaction of an Air System with Concrete Core Conditioning." *Energy and Buildings* 30(2): 139–45.

Li, Deyang, and Zhihuan Song. 2020. "A Novel Incremental Gaussian Mixture Regression and Its Application for Time-Varying Multimodal Process Quality Prediction." In *2020 IEEE 9th Data Driven Control and Learning Systems Conference (DDCLS)*, , 645–50.

Liu, Kuixing et al. 2011. "Establishment and Validation of Modified Star-Type RC-Network Model for Concrete Core Cooling Slab." *Energy and Buildings* 43(9): 2378–84.

Neumann, Hannah, Sebastian Gamisch, and Stefan Gschwander. 2021. "Comparison of RC-Model and FEM-Model for a PCM-Plate Storage Including Free Convection." *Applied Thermal Engineering* 196: 117232.

O'Dwyer, Edward et al. 2016. "Modelling and Disturbance Estimation for Model Predictive Control in Building Heating Systems." *Energy and Buildings* 130: 532–45.

Rhee, Kyu-Nam, and Kwang Woo Kim. 2015. "A 50 Year Review of Basic and Applied Research in Radiant Heating and Cooling Systems for the Built Environment." *Building and Environment* 91: 166–90.

Rodríguez Jara, Enrique Á. et al. 2016. "A New Analytical Approach for Simplified Thermal Modelling of Buildings: Self-Adjusting RC-Network Model." *Energy and Buildings* 130: 85–97.

Sourbron, M. et al. 2009. "Efficiently Produced Heat and Cold Is Squandered by Inappropriate Control Strategies: A Case Study." *Energy and Buildings* 41(10): 1091–98.

Sung, Hsi Guang. 2004. "Gaussian Mixture Regression and Classification." Ph.D. Rice University. https://www.proquest.com/docview/305155652/abstract/8C63788CCF824897PQ/1 (April 12, 2022).

Wang, Liping, Robert Kubichek, and Xiaohui Zhou. 2018. "Adaptive Learning Based Data-Driven Models for Predicting Hourly Building Energy Use." *Energy and Buildings* 159: 454–61.

Zhang, Rui, Khee Poh Lam, Shi-chune Yao, and Yongjie Zhang. 2013. "Coupled EnergyPlus and Computational Fluid Dynamics Simulation for Natural Ventilation." *Building and Environment* 68: 100–113.